Optics Letters

GaN/AlN quantum-disk nanorod 280 nm deep ultraviolet light emitting diodes by molecular beam epitaxy

TONGBO WEI,[1,4,†] S. M. ISLAM,[2,†] UWE JAHN,[3] JIANCHANG YAN,[1] KEVIN LEE,[2] SHYAM BHARADWAJ,[2] XIAOLI JI,[1] JUNXI WANG,[1] JINMIN LI,[1] VLADIMIR PROTASENKO,[2] HUILI (GRACE) XING,[2] AND DEBDEEP JENA[2,*]

[1]Semiconductor Lighting R&D center, Institute of Semiconductors, Chinese Academy of Sciences, Beijing 100083, China
[2]Deparment of Electrical and Computer Engineering, Cornell University, Ithaca, New York 14853, USA
[3]Paul-Drude-Institut fürFestköperelektronik, Hausvogteiplatz 5-7, 10117 Berlin, Germany
[4]e-mail: tbwei@semi.ac.cn
*Corresponding author: djena@cornell.edu

Received 4 July 2019; revised 8 November 2019; accepted 12 November 2019; posted 20 November 2019 (Doc. ID 371716); published 19 December 2019

We report optically and electrically pumped ∼280 nm deep ultraviolet (DUV) light emitting diodes (LEDs) with ultra-thin GaN/AlN quantum disks (QDs) inserted into AlGaN nanorods by selective epitaxial regrowth using molecular beam epitaxy. The GaN/AlN QD LED has shown strong DUV emission distribution on the ordered nanorods and high internal quantum efficiency of 81.2%, as a result of strain release and reduced density of threading dislocations revealed by transmission electron microscopy. Nanorod assembly suppresses the lateral guiding mode of light, and light extraction efficiency can be increased from 14.9% for planar DUV LEDs to 49.6% for nanorod DUV LEDs estimated by finite difference time domain simulations. Presented results offer the potential to solve the issue of external quantum efficiency limitation of DUV LED devices. © 2019 Optical Society of America

https://doi.org/10.1364/OL.45.000121

AlGaN-based deep ultraviolet (DUV) light emitting diodes (LEDs) are in strong demand, including sterilization and biochemical detection. However, AlGaN LEDs emitting in the window of 200–280 nm still suffer from low external quantum efficiency (EQE), typically less than 10% for 280 nm LEDs and drops down further to ∼1% for emission wavelengths below 250 nm [1,2]. The severe degradation of UV light in the C spectrum (UV-C) LEDs is attributed to high dislocation densities, poor hole transport, and low light extraction efficiency (LEE) [3,4]. Numerous efforts have been made to improve the material quality and to enhance the hole injection, such as epitaxy on bulk AlN substrate [5,6], using nano-patterned sapphire substrates [7] and polarization-induced doping [8,9]. However, LEE of DUV LEDs has been typically limited to ∼10% [10], primarily due to absorption within the Ga(Al)N p-contact layer and, more importantly, to the optical polarization properties of AlGaN quantum wells (QWs). AlGaN QWs emit light with both transverse electric (TE) and transverse magnetic (TM) polarization. With the increase of Al composition in AlGaN QWs, light propagation direction gradually changes from surface emitting TE to edge emitting TM [11], which results in severe internal reflection. Extraction of light from the surface becomes challenging for QWs for sub-280-nm emission.

As an alternative to AlGaN, ultra-thin GaN quantum dots and wells for short wavelength LEDs have been explored over the last few years [12]. Using high quantum confinement and the large band offset between AlN and GaN, a few monolayer (ML) GaN quantum structures can tune light emission wavelengths from 365 nm to 232 nm, even further down to 222 nm for 1–2 ML-thick GaN quantum dots [13]. Thus, ultra-thin GaN/AlN quantized structures address the optical selection rule problem [14], improving light extraction compared to AlGaN active regions. Furthermore, three-dimensional (3D) carrier confinement in GaN quantum dots of the active region also helps to suppress non-radiative recombination resulting in further enhancement of internal quantum efficiency (IQE) [15].

So far, it remains extremely challenging to realize high-efficiency ultra-thin GaN quantum dot DUV LEDs with planar structures due to the small critical angle of around 23° at the interface. Recent studies have shown that self-organized AlGaN nanowires can potentially improve the efficiency of UV-C LEDs [16]. High LEE can be made by redirecting trapped light into a radiated mode from nanowires. However, there have been only few reports on 3D nanostructure DUV LEDs using GaN as the active region [17]. The exploration of performance and underlying physics of such an active region is still lacking. In this letter, we demonstrate a design of a GaN/AlN quantum-disk (QD) nanorod DUV LED by selective epitaxial regrowth on ordered AlGaN nanorod arrays using molecular beam epitaxy (MBE). DUV emission of ∼280 nm from 3D GaN disks in an AlN matrix is excited both optically and electrically. The

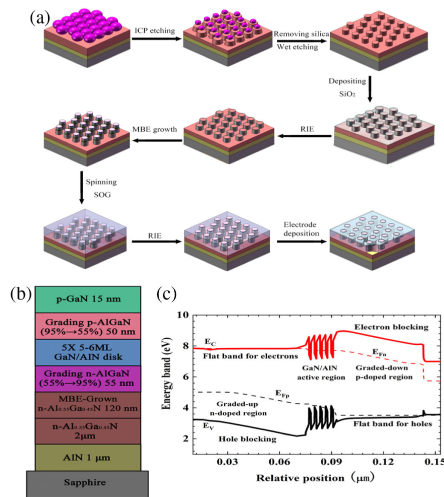

Fig. 1. Schematic diagram of (a) fabrication process flow and (b) layer structures of the GaN/AlN QD nanorod DUV LED. (c) Simulated energy band diagram of the nanorod DUV LED at 50 A/cm^2.

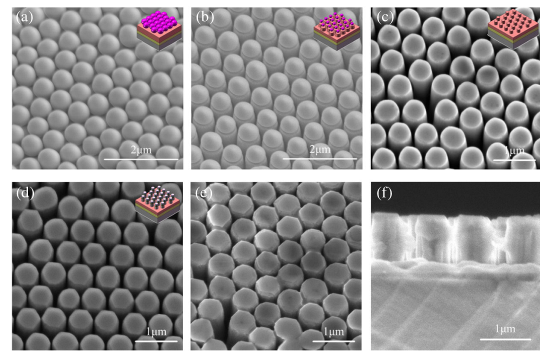

Fig. 2. SEM images of (a) AlGaN wafer covered with a monolayer of self-assembled silica nanospheres, AlGaN nanorod arrays (b) with and (c) without silica nanospheres after ICP etching. (d) GaN/AlN active region grown by MBE on AlGaN nanorods. The inset shows the schematic process step. (e) Tilted view and (f) cross-section view of the full structure DUV LED on nanorods.

GaN/AlN QD nanorod LED exhibits high IQE, nearly 81.2%. By simulations, the LEE of nanorod DUV LED is estimated to be 49.6%, attributing to the suppressed lateral guide and diffraction and scatting between nanorods and air.

The growth and fabrication process to realize the GaN/AlN QD nanorod DUV LED were depicted in Fig. 1(a). First, a 1-μm-thick AlN layer and a 2-μm-thick $Al_{0.55}Ga_{0.45}N$ layer were grown on a *c*-plane sapphire using a home-made metal-organic chemical vapor deposition (MOCVD). Second, a highly ordered self-assembled ML of silica nanospheres was dip-coated on an AlGaN surface [18]. Then, the nanospheres were utilized as masks in an inductively coupled plasma (ICP) dry etching process. Wet etching in a KOH-based etchant, AZ400K, was carried out for 3 min to eliminate the ICP-induced damage. To passivate the nanorod sidewalls, a 10-nm-thick SiO_2 layer was deposited onto the overall surface using plasma enhanced chemical vapor deposition (PECVD). Then, the reactive ion etching (RIE) process was employed to expose AlGaN on the top of the nanorods. Due to the different etching rates between the top and sidewall, SiO_2 on the surface of the nanorod sidewall remained after the etching. The AlGaN nanorod was loaded into a Veeco Gen 930 RF plasma MBE to complete the DUV LED growth. Figure 1(b) shows the structure of the DUV LEDs on AlGaN nanorods. A *n*-$Al_{0.55}Ga_{0.45}N$ layer was grown followed by a compositionally graded *n*-AlGaN region from 55% to 95%. For the DUV emitting region, five periods of GaN/AlN QDs were grown on AlGaN nanorods with a N-rich active flux ratio Ga/N < 1 at 700°C using the Stranski–Krastanov (SK) method. The GaN thickness was kept to about 5–6 MLs, and the AlN barrier thickness was kept at 2 nm. More growth details can be found in our previous paper [19]. The simulated energy band diagram of a single GaN/AlN QD nanorod using APSYS at a forward current of 50 A/cm^2 is shown in Fig. 1(c). The graded layers produce the effective electron and hole blocking to help radiative recombination in the GaN/AlN active region. The flat bands in the carrier injection layers ensure smooth carrier transport up to the active region, followed by tunnel injection.

To fabricate the DUV nanorod LED device, spin-on glass (SOG) was then spun on the surface of the nanorod arrays to planarize the surface. After curing the SOG at 400°C for 20 min, the gap between nanorods was filled with SOG. Then, the SOG was etched by RIE to expose the top portion of nanorods, while the sidewall of the nanorods was still covered with SOG. A Ti (20 nm)/Al (100 nm)/Ni (40 nm)/Au (50 nm) metal stack was evaporated on the *n*-AlGaN layer and Ni (5 nm)/Au (5 nm) was evaporated on the *p*-type layer as a current spreading layer followed by a circular Ti (20 nm)/Au (100 nm) probe pad with a diameter of 50 μm. Finally, after the thermal annealing, GaN/AlN QD nanorod LED devices with a mesa area of 200 μm × 200 μm were obtained.

Tilted scanning electron microscopy (SEM) images of silica nanospheres before and after ICP etching are shown in Figs. 2(a) and 2(b). The hexagonal close-packed nanospheres as the mask exhibit a diameter of 600 nm. When the etch depth of AlGaN reaches 800 nm, highly uniform silica nanospheres remain on top of the AlGaN nanorods with an ellipsoidal shape, whose diameters are equal to that of AlGaN nanorods. After removing the nanospheres and eliminating ICP damage, highly ordered and truncated cone-shaped nanorod arrays are well produced with damage-free surface, as shown in Fig. 2(c). The anisotropic wet etching in AZ400K has a relatively fast etch rate in the $(10\bar{1}0)$ *m*-plane sidewalls of AlGaN nanorods, while there is almost no etch on the *c*-plane top surface. Here, the diameter of the cone-shaped AlGaN nanorod top is about 500 nm, nearly equal to the bottom diameter of nanorods. The spacing between nanorods is about 100 nm, which may be tuned by changing the duration time of the wet etching. Figure 2(d) shows the GaN/AlN QD active region grown on the AlGaN nanorods by MBE. The *n*-AlGaN and subsequent GaN/AlN QD active region are confined on the top of nanorods with a flat surface. In contrast, the gap between nanorods becomes smaller following the growth *p*-AlGaN and *p*-GaN from the tilted and cross-section view of LEDs in Figs. 2(e) and 2(f). The incorporation of Mg leads to a relative enhancement of the lateral growth rate, which is estimated to be $\sim$1 nm min^{-1}.

Figure 3(a) shows the cross-section transmission electron microscopy (TEM) image of the QD DUV LED on nanorods. One can clearly recognize the regrown AlGaN interface by

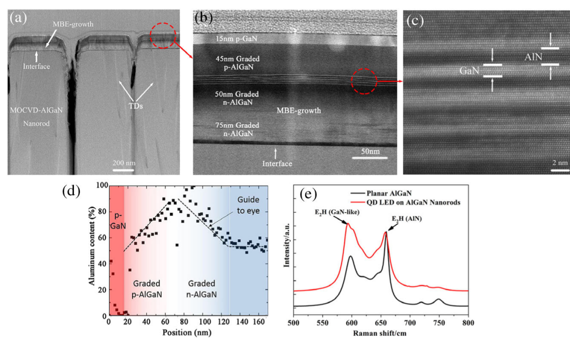

Fig. 3. (a) Cross-section TEM image of the GaN/AlN QD nanorod LED. HAADF-STEM images of an (a) isolated nano-rod, (b) zoomed view of the MBE-grown LED structure, (c) five periods of GaN/AlN active region, and (d) EDX compositional profile of Al confirming desired heterostructure. (e) Raman spectra measured from planar AlGaN and QD nanorod LED.

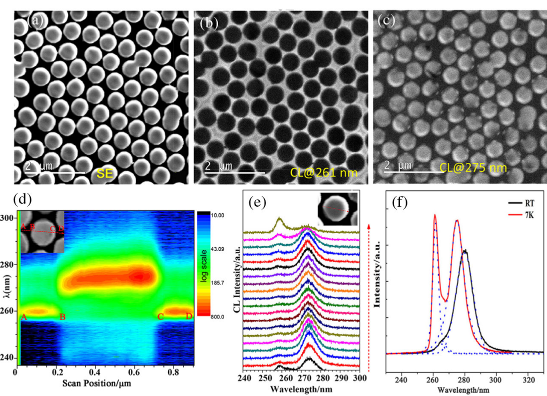

Fig. 4. (a) SEM of GaN/AlN QD nanorod LED. (b) and (c) Corresponding monochromatic CL images at 7 K for detection wavelengths of 261 and 275 nm. (d) 2D representation of a CL spectral line scan intersecting an individual nanorod with the intensity color coded in a logarithmic scale. (e) CL spectra along a line crossing a single nanorod (cf. Inset) at 7 K. (f) CL spectra of GaN/AlN QD nanorod LED at RT and 7 K.

MBE. Some threading dislocations (TDs) propagating from the MOCVD-grown AlGaN layer also terminate at the interface on nanorods. For the active regions of the nanorod LED, high-angle annular dark-field scanning TEM (HAADF-STEM) images are presented in Figs. 3(b) and 3(c). The first two periods of the desired GaN/AlN heterostructures are altered by the presence of excess Ga from the metal-rich growth of the n-AlGaN cladding region. In fact, the active region is roughly composed of a $5x\mathrm{Al}_{0.15}\mathrm{Ga}_{0.85}\mathrm{N}/\mathrm{Al}_{0.85}\mathrm{Ga}_{0.15}\mathrm{N}$ heterostructure as resolved from the TEM energy dispersive x-ray spectroscopy (EDX) analysis in Fig. 3(d). We hypothesize that the fast migration of Ga adatoms to the top of the nanorod compared to the Al adatoms in the Ga-rich condition results in the intermixing of Al and Ga to form AlGaN barriers. The non-uniformity of the thickness and composition of the first $2x$ AlGaN/AlGaN layers are also a consequence of the fast migration of accumulated Ga adatoms along the sidewall of the nanorods. Micro-Raman measurement of the nanorod LEDs was also performed to evaluate the stress distribution in Fig. 3(e). The Raman phonon modes, E_2H (GaN-like) and E_2H (AlN), of the GaN/AlN QD nanorod LED are located at approximate 593.3 cm^{-1} and 657.4 cm^{-1}, respectively. In contrast, the corresponding values are 598.1 cm^{-1} and 659.3 cm^{-1} for that on planar AlGaN. The obvious shifts of E_2H (GaN-like) and E_2H (AlN) phonon lines toward the high-frequency side are indications of the relaxation of compressive stress in the nanorod DUV LED.

The spatial emission of the GaN/AlN QD nanorod LED is investigated by the cathodoluminescence (CL) at 7 K using an acceleration voltage of 3 kV. A plane-view SEM image is first shown in Fig. 4(a). Monochromatic CL images acquired for detection wavelengths of 261 and 275 nm are presented in Figs. 4(b) and 4(c), respectively. The CL spectrum exhibits two strong peaks, as shown in Fig. 4(f). The emission pattern fully follows the nanorod contour distribution. The emission at 261 nm is localized at the gaps between the nanorods, originating from the underlying AlGaN. The full width at half-maximum (FWHM) of this emission line is 4.1 nm. The CL intensity of another strong emission peak is centered at 275 nm and exhibits a FWHM of 10.4 nm. It is quite uniformly distributed on the top of the nanorods, indicating a homogeneous distribution of GaN/AlN QDs within the active region. Figure 4(d) shows a two-dimensional (2D) representation of a CL spectral line scan intersecting an individual nanorod with the intensity color coded, which is consistent with the mapping profile. Additionally, Fig. 4(e) shows a CL line scan along the red dashed line across the nanorod top with a step length of 30 nm. The CL emission at 275 nm originating from the top of the nanorod does not show an obvious spectral shift along the probed path way. A CL peak centered at about 260 nm appears only when approaching the gap between the nanorods. As temperature is increased to room temperature (RT), only the GaN/AlN QDs-related emission can be observed showing a red shift toward 280 nm [cf. Fig. 4(f)]. The ICP damage of AlGaN leads to a rapid deterioration of the corresponding emission at 261 nm with an increase of the temperature. Roughly, IQE may be evaluated by comparing photoluminescence (PL) intensities, assuming IQE is 100% at low temperature (LT) regardless of excitation carrier density [20]. Here, the IQE of the GaN/AlN QD nanorod DUV LED reaches 81.2% by comparing CL intensity at RT and 7 K. Such high IQE value of DUV LEDs is attributed to a reduced density of TDs and to a released strain in the GaN/AlN QD active region during selective epitaxial regrowth.

Figure 5(a) shows the RT PL spectra of AlGaN nanorods and GaN/AlN QD nanorod DUV LEDs, excited by a 157 nm pulsed excimer laser. Compared to the narrow emission of 265 nm from AlGaN nanorods, the GaN/AlN QD LED exhibits wide emission dominated at 279 nm. Two shoulder peaks below 270 nm are attributed to the emission from underlying AlGaN and graded AlGaN layers. Figure 5(b) shows the experimental and simulated electroluminescence (EL) spectra of the GaN/AlN QD DUV LED at current density of 50 $\mathrm{A/cm}^2$ under pulsed excitation at 10 kHz and 5% duty cycle. For a current of 20 mA, the voltage of the GaN/AlN QD nanorod LED is 12.6 V due to sub-ohmic p contacts on the nanorod top. The emitted light is collected from the device top surface with an optical fiber. A strong EL peak can be observed at 275 nm, accompanied by a shoulder peak at 260 nm. The weak shoulder

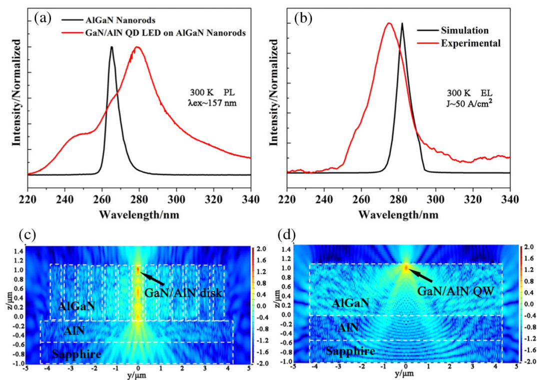

Fig. 5. (a) RT PL spectra from AlGaN nanorods and GaN/AlN QD nanorod DUV LEDs. (b) Experimental and simulated EL of the GaN/AlN QD DUV LED at 50 A/cm^2. FDTD simulation of light propagation of (c) QD nanorod LED and (d) QW LED on planar AlGaN.

peak may originate from the recombination at *p*-AlGaN, due to the overflow of electrons from the active region. The APSYS simulation is performed for the composition of the active region and GaN thickness of ~1 nm obtained from TEM. The simulated and experimental EL emission is consistent, but there is a large discrepancy in the line shapes. Compared to the simulation result, the peak blue shift of the GaN/AlN QD LED on nanorods may be caused by the fast diffusivity of Al and Ga atoms at the low-strain state in the active region, which results in partial formation of the AlGaN QD active region. Another shift reason is the limitations of band structure at high conduction and valence band energies in the theory. GaN thickness fluctuation in experiments also leads to the broadening of the EL peak.

To understand the light propagation in the nanorod LED, 3D finite difference time domain (FDTD) simulations were performed. To simplify the numerical computations, the lateral dimension of the nanorod DUV LED model is set as 8×8 μm. The dipole source is polarized in the direction parallel to the in-plane for the excitation of the TE mode. A monitor is set above the model to detect the light emitted from the top surface. Another four monitors are around the model to detect the light emitted from the sidewall. Then, the LEE is defined as the ratio of the sum of the light power tested by the top and around the monitors to the total power from the dipole source. Figures 5(c) and 5(d) compare the propagation of electromagnetic waves passing through the GaN/AlN QD nanorod LED and planar QW LED. It is obvious that the light emitted from top surface of the nanorod LED is far more than that of the planar LED because the nanorod structure changes the wave guide mode and overcomes the total internal reflection. Hence, many guided modes in planar LEDs become the leaky modes in nanorod LEDs through diffraction and scattering. Undoubtedly, the weaker distribution of the electric field is around the nanorod LED than around the planar LED because most of the light is extracted from the top surface of the nanorod LED. As a result, the corresponding LEE may be increased from 14.9% for the planar LED to 49.6% for the nanorod LED. Therefore, the GaN/AlN QD nanorod DUV LED is beneficial for realizing high IQE and LEE simultaneously.

In summary, a novel design of the highly uniform GaN/AlN QD DUV LED is accomplished by selective epitaxial regrowth on ordered AlGaN arrays using MBE. Strong DUV emission of ~280 nm from the GaN disk is detected both optically and electrically. CL mapping shows uniform emission at 275 nm with 10.4 nm FWHM on the top of the nanorods. Due to strain release and a reduction of TD density, the GaN/AlN QD DUV LED has shown a higher IQE of ~81.2%. In addition, the periodic arrays of the nanorod LED lead to an enhancement of LEE from 14.9% for the planar structure to 49.6% estimated by FDTD simulations.

Funding. National Key R&D Program of China (2018YFB0406703); National Science Foundation (1710298); Division of Materials Research (1338010).

†These authors contributed equally to this work.

REFERENCES

1. M. Kneissl and J. Rass, *III-Nitride Ultraviolet Emitters* (Springer, 2016).
2. T. Takano, T. Mino, J. Sakai, N. Noguchi, K. Tsubaki, and H. Hirayama, Appl. Phys. Express **10**, 031002 (2017).
3. B. Cheng, S. Choi, J. E. Northrup, Z. Yang, C. Knollenberg, M. Teepe, T. Wunderer, C. L. Chua, and N. M. Johnson, Appl. Phys. Lett. **102**, 231106 (2013).
4. B. H. Le, S. Zhao, X. Liu, S. Y. Woo, G. A. Botton, and Z. Mi, Adv. Mater. **28**, 8446 (2016).
5. Z. Bryan, I. Bryan, J. Xie, S. Mita, Z. Sitar, and R. Collazo, Appl. Phys. Lett. **106**, 142107 (2015).
6. J. R. Grandusky, J. Chen, S. R. Gibb, M. C. Mendrick, C. G. Moe, L. Rodak, G. A. Garrett, M. Wraback, and L. J. Schowalter, Appl. Phys. Express **6**, 032101 (2013).
7. H. Chang, Z. Chen, W. Li, J. Yan, R. Hou, S. Yang, Z. Liu, G. Yuan, J. Wang, J. Li, P. Gao, and T. Wei, Appl. Phys. Lett. **114**, 091107 (2019).
8. J. Simon, V. Protasenko, C. Lian, H. Xing, and D. Jena, Science **327**, 60 (2010).
9. Y. Zhang, S. Krishnamoorthy, J. M. Johnson, F. Akyol, A. Allerman, M. W. Moseley, A. Armstrong, J. Hwang, and S. Rajan, Appl. Phys. Lett. **106**, 141103 (2015).
10. M. Ichikawa, A. Fujioka, T. Kosugi, S. Endo, H. Sagawa, H. Tamaki, T. Mukai, M. Uomoto, and T. Shimatsu, Appl. Phys. Express **9**, 072101 (2016).
11. T. Kolbe, A. Knauer, C. Chua, Z. Yang, S. Einfeldt, P. Vogt, N. M. Johnson, M. Weyers, and M. Kneissl, Appl. Phys. Lett. **97**, 171105 (2010).
12. Y. Taniyasu and M. Kasu, Appl. Phys. Lett. **99**, 251112 (2011).
13. J. Verma, P. K. Kandaswamy, V. Protasenko, A. Verma, H. Xing, and D. Jena, Appl. Phys. Lett. **102**, 041103 (2013).
14. C. Liu, Y. K. Ooi, S. M. Islam, J. Verma, H. Xing, D. Jena, and J. Zhang, Appl. Phys. Lett. **110**, 071103 (2017).
15. J. Renard, P. K. Kandaswamy, E. Monroy, and B. Gayral, Appl. Phys. Lett. **95**, 131903 (2009).
16. S. Zhao, M. Djavid, and Z. Mi, Nano Lett. **15**, 7006 (2015).
17. A. T. M. G. Sarwar, B. J. May, M. F. Chisholm, G. J. Duscher, and R. C. Myers, Nanoscale **8**, 8024 (2016).
18. C. Geng, L. Zheng, J. Yu, Q. Yan, T. Wei, X. Wang, and D. Shen, J. Mater. Chem. C **22**, 22678 (2012).
19. S. M. Islam, K. Lee, J. Verma, V. Protasenko, S. Rouvimov, S. Bharadwai, H. Xing, and D. Jena, Appl. Phys. Lett. **110**, 041108 (2017).
20. S. Watanabe, N. Yamada, M. Nagashima, Y. Ueki, C. Sasaki, Y. Yamada, T. Taguchi, K. Tadatomo, H. Okagawa, and H. Kudo, Appl. Phys. Lett. **83**, 4906 (2003).

132.236.27.111 {ts 2019-12-17 20:47:08}